

Monitoring the Progress and Healing Status of Burn Wounds Using Infrared Spectroscopy

Applied Spectroscopy
2020, Vol. 74(7) 758–766
© The Author(s) 2020
Article reuse guidelines:
sagepub.com/journals-permissions
DOI: 10.1177/0003702820919446
journals.sagepub.com/home/asp



Pedro A.A. Castro¹ , Cassio A. Lima^{1,2}, Mychel R.P.T. Morais³,
Telma M.T. Zorn³, and Denise M. Zezell¹ 

Abstract

Burns are one of the leading causes of morbidity worldwide and the most costly traumatic injuries. A better understanding of the molecular mechanisms in wound healing is required to accelerate tissue recovery and reduce the health economic impact. However, the standard techniques used to evaluate the biological events associated to wound repair are laborious, time-consuming, and/or require multiple assays/staining. Therefore, this study aims to evaluate the feasibility of Fourier transform infrared (FT-IR) spectroscopy to monitor the progress and healing status of burn wounds. Burn injuries were induced on Wistar rats by water vapor exposure and biopsied for further histopathological and spectroscopic evaluation at four time-points (3, 7, 14, and 21 days). Spectral data were preprocessed and compared by principal component analysis. Pairwise comparison of post-burn groups to each other revealed that metabolic activity induced by thermal injury decreases as the healing progresses. Higher amounts of carbohydrates, proteins, lipids, and nucleic acids were evidenced on days 3 and 7 compared to healthy skin and reduced amounts of these molecular structural units on days 14 and 21 post-burn. FT-IR spectroscopy was used to determine the healing status of a wound based on the biochemical information retained by spectral signatures in each phase of healing. Our findings demonstrate that FT-IR spectroscopy can monitor the biological events triggered by burn trauma as well as to detect the wound status including full recovery based on the spectral changes associated to the biochemical events in each phase.

Keywords

Infrared spectroscopy, burn, wound healing, principal component analysis, PCA

Date received: 6 November 2019; accepted: 17 March 2020

Introduction

Burns are a global public health problem and one of the leading causes of morbidity worldwide. An estimated 180000 deaths every year are caused by burns, in which the vast majority occur in low- and middle-income countries.¹ Due to the extensive time of hospitalization, rehabilitation, treatment of wounds and scars, burns are the most costly traumatic injuries.^{2,3}

After a burn trauma, a complex cascade of events is triggered in order to recover the tissue stability. The wound healing process is divided into four distinct and overlapped phases known as homeostasis, inflammation, proliferation, and remodeling.^{4,5} Deregulation of one of these phases might alter the normal repair process, resulting in impaired healing (chronic hard-to-heal ulcers or excessive scarring).^{6,7} In order to accelerate the wound repair/regeneration process, a better understanding of the cellular and molecular mechanisms underlying wound healing is

necessary. However, the biological events involved in tissue repair as well as its failure to heal are still not fully understood.^{8,9}

Determining the healing status of a wound after a burn trauma plays an important role in deciding on a suitable treatment regimen. The techniques routinely used to

¹Instituto de Pesquisas Energeticas e Nucleares (IPEN-CNEN/SP), University of Sao Paulo (USP), Sao Paulo, Brazil

²Department of Biochemistry, Institute of Integrative Biology, University of Liverpool, Liverpool, UK

³Instituto de Ciencias Biomedicas (ICB), University of Sao Paulo (USP), Sao Paulo, Brazil

Corresponding author:

Denise M. Zezell, Instituto de Pesquisas Energeticas e Nucleares (IPEN-CNEN/SP), University of Sao Paulo (USP), Av. Lineu Prestes, 2242, 05508-000 Sao Paulo, Brazil.

Email: zezell@usp.br

study the mechanisms of wound tissue repair may include histological examination of tissue biopsies, immunohistochemistry, in situ hybridization, polymerase chain reaction, etc.^{10–12} These methods are expensive, laborious, time-consuming, and require multiple assays/stains. Thus, new technologies that are able to determine the healing status of a wound as well as to provide information for a better understanding of the wound repair process in a simple and fast way have been investigated over the last years. Infrared spectroscopy and several other optical methods have been proposed for the characterization of physical and chemical properties of skin.^{13–19} Fourier transform infrared (FT-IR) spectroscopy provides information about the overall biochemical status of the examined sample based on the vibrations of molecular structural units (lipids, proteins, nucleic acids, and carbohydrates) that are infrared active.²⁰ The potential applications of FT-IR spectroscopy as a tool to study biological samples has been well demonstrated over the past years. Most studies have focused on using the biochemical information retained by spectral data for the diagnosis of cancerous and non-cancerous diseases,^{21–25} as well as to evaluate drug–disease interaction.^{6,26–29} However, the molecular vibrations measured by FT-IR spectroscopy also provides valuable information which can be used for analyzing basic biological processes, such as cell division and death mechanisms,^{30,31} presenting a great promise as a tool to assess biological events triggered by wound repair.^{32–35} In light of this, this study aims to evaluate the feasibility of FT-IR spectroscopy to monitor the progress and healing status of burn wounds based on the spectral changes associated to the biochemical events in each healing phase.

Materials and Methods

Animal Experiment and Sample Preparation

After approval by the institutional Ethics Committee for Animal Research (CEUA IPEN 165/15), burn injuries were induced on the back of Wistar rats by applying water vapor at 90 °C for 12 s.^{36,37} Tissue specimens were extracted after 3, 7, 14, and 21 days of thermal injury, as shown in Table I, in order to evaluate the progress and

Table I. Experimental setup.

Group	Post-burn days	No. of rats	No. of tissue specimen	No. of spectra collected per group
G0	–	5	25	60
G1	3	10	40	65
G2	7	10	25	60
G3	14	10	25	30
G4	21	10	25	70

healing status of the wound repair. The specimens were cryopreserved, and longitudinally oriented sections of 5 μm thickness were placed in MirrIR low-E-coated slides (Kevley Technologies, Chesterland, OH). Previous studies have reported the occurrence of an electric field standing wave artifact in thin samples placed onto low-E coated slides, which may induce spectral distortions such as alterations in the peak shape and position.^{38–42} According to Cui et al.,⁴³ tissue sections thicker than 2–3 μm should be used in order to avoid undesirable spectral distortions. Thus, in the present study, spectral data were acquired from tissue sections of 5 μm thickness. More than one biopsy was taken from each animal, according to ethical committee guidelines.

FT-IR Spectroscopy

Spectral data were collected using an FT-IR system (Thermo Nicolet 6700, Waltham, MA) operating with an attenuated total reflectance accessory as sampling mode (Smart Orbit, Thermo Scientific, Waltham, MA). Measurements were performed in MID-infrared region (4000–400 cm^{-1}) with spectral resolution of 4 cm^{-1} and 150 scans per spectrum in which tissue specimens were pressed into a diamond crystal with an area of 2.25 mm^2 . Spectral collections were performed in a random mapping point-by-point in the entire tissue biopsy.¹⁵ Up to 10 spectra were measured in each tissue biopsy. Each spectrum obtained represents the equidistant measurement in each biopsy. After that, a spectral quality control was performed.

Chemometric Analysis

Fingerprint region (900–1800 cm^{-1}) and high wavenumber region (2800–3000 cm^{-1}) were truncated for posterior offset–correction and normalized by amide I band area. Second derivatives were calculated from spectra in order to assess the overlapped sub-bands and smoothed by Savitzky-Golay filter with a polynomial of second order in a 13–point window. Spectra collected from healthy tissue over the range of 1000–1400, 1500–1800, and 2800–3000 cm^{-1} were compared to burn injuries using principal component analysis (PCA).^{20,44} More information about the selection of spectral range used as input for PCA is provided in the supplemental material, in which accuracy, sensitivity, and specificity are showed according to the healing stage (supplementary Appendix—PCA performance). For chemometric validation, we compare the PCA results with spectral barcodes based on Mann–Whitney U-test.⁴⁵ A complete description of these evaluations is shown in the Supplemental Material (Appendix—Chemometric Validation). All chemometric methods, including the average spectrum and standard deviation from each group according to post-burn days, were carried out on Matlab R2015a (MathWorks, Natick, MA).

Results

Histological Evaluation

Figure 1 shows histological sections of the skin tissue before and after the burn experiment. The healthy skin showed a typical histological organization: an outer epidermis formed by a thick squamous stratified epithelium and an underlying dermis composed of dense connective tissue (Fig. 1a).

On day 3 post-burn (Fig. 1b), the integrity of the skin tissue was strikingly altered. The burn-wound lacked the characteristic squamous stratified epithelium, and the underneath dermis exhibited dense bundles of collagen fibers. Prominent granulation tissue was observed in the dermis wherein a wide inflammatory cell infiltration could be identified. On day 7 post-burn (Fig. 1c), areas of re-epithelization were observed on the surface of the burn-wound, and the remodeling of dermis subjacent to the burn-wound was still ongoing as dense bundles of collagen fibers was observed in a random orientation. It was observed that there was a noticeable decrease in the extension of granulation tissue and the number of inflammatory cells in the dermis compared to the previous stage. On day 14 post-burn (Fig. 1d), re-epithelization was advanced. The new epithelial layer completely covered the burn-wound surface and exhibited intense cell proliferative activity in its basal domain. Moreover, a distinct albeit discrete corneal stratum was observed in the apical surface of the newly formed epithelium. The subjacent dermis displayed a loose connective tissue wherein numerous fibroblasts were observed (Fig. 1d). Neither granulation tissue nor

inflammatory cell infiltrate was observed in the healing tissue at this stage. On day 21 post-burn (Fig. 1e), the healing burn-wound was fairly comparable to the healthy skin in terms of histological organization. The epidermis and dermis were completely re-stored and the skin surface was entirely covered by a typical squamous stratified epithelium.

FT-IR Spectroscopy

Figure 2 shows the averages of spectra and second derivatives of healthy and post-burn wounds at different days over the range of $1000\text{--}4000\text{ cm}^{-1}$. Spectral regions over $1400\text{--}1500\text{ cm}^{-1}$ and $1800\text{--}2800\text{ cm}^{-1}$ were excluded prior spectroscopic analysis.

According to Fig. 2, alterations on band peak position as well as the appearance or disappearance of infrared bands were not observed between the groups. The vibrational modes are identified on the second derivatives and their biological assignments are summarized in Table II.

Differences in healthy tissue to skin submitted to thermal injury measurements were compared using PCA in order to monitor the biochemical changes induced by the healing process in each time-point (3, 7, 14, and 21). Figures 3a and 3c show score plots using the first (PC1) and second (PC2) principal components obtained for G0 compared to G1 and G2. Satisfactory data discrimination was achieved in both cases along PC1, in which most scores from G1 and G2 are grouped on negative values of PC1 axis, and scores from G0 lie in the positive values. Figures 3b and 3d depict the loadings associated to PC1 in each

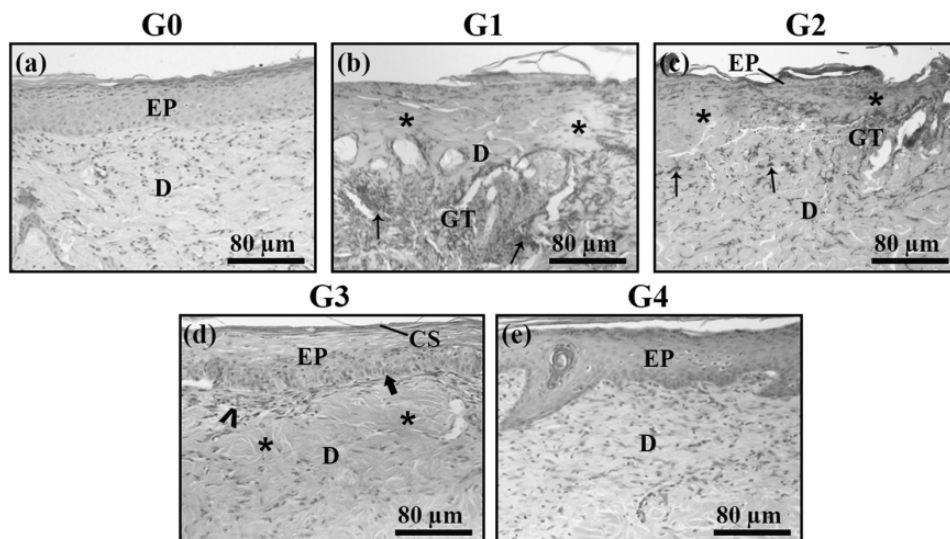


Figure 1. Representative photomicrographs of healthy skin (a) and burn-wound during the healing process (b–e). (b) day 3 post-burn; (c) day 7 post-burn; (d) day 14 post-burn; (e): day 21 post-burn. EP: epidermis; D: dermis; GT: granulation tissue; CS: corneal stratum; thin arrow—inflammatory infiltrate; *Dense collagen bundles; Loose connective tissue; large arrow is epithelial proliferative area. Hematoxylin and Eosin staining. $100\times$ magnification.

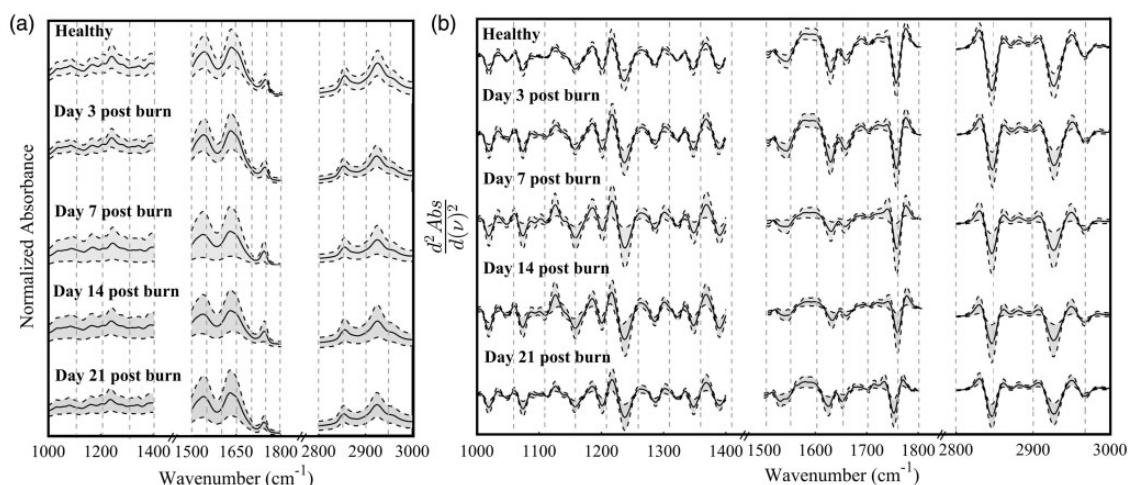


Figure 2. Averages and standard deviation of spectra (a) and second derivatives (b) of healthy and post-burn wounds at different days of healing process over the range 1000–3000 cm^{-1} .

Table II. Biological assignments for vibrational modes observed in the second derivative of averaged spectra.

Band (cm^{-1})	Assignment	References
1029	Carbohydrates	46,47
1082	Carbohydrates and nucleic acids	46,47
1202	Proteins	46,47
1235	Proteins and nucleic acids	46–48
1280	Proteins	46,47
1340	Proteins	46,48
1626	Proteins	46–48
1653	Proteins	46,47
1745	Lipids	46,47
2852	Lipids	46,47,49
2924	Lipids	46,47,49

pairwise comparison and retain information about the variables responsible by different groupings along PC1 axis in the score plots. Considering that PCA was applied on the second derivatives, positive scores are related to negative loadings and negative scores are related to positive loadings.

In both cases, positive loadings were evidenced for all vibrational modes, indicating an increase in the amount of carbohydrates (1028 and 1082 cm^{-1}), proteins (1202, 1235, 1280, 1340, 1626, and 1653 cm^{-1}), and lipids (1745, 2852, and 2924 cm^{-1}) in the tissue from groups thermally injured.

Figures 4a and 4c depict scores plots (PC1 \times PC2) obtained for G0 compared to spectral data collected from G3 and G4. Scores associated with spectra from G0 lie on the negative values of PC1, whereas scores from G3

and G4 are grouped on positive values. Loadings of PC-1 (Figs. 4b and 4d) indicated a decrease in the amount of carbohydrates, proteins, lipids, and nucleic acids in the post-burn groups.

Spectral data from groups submitted to thermal injury were also compared to each other in order to evaluate the metabolic activity during the healing process. PCA scores obtained comparing spectral data from G1 to G3 and G4 groups are shown in Figs. 5a and 5c, in which the first principal component provided satisfactory data discrimination. Loadings of PC1 from each pairwise comparison are shown in Figs. 5b to 5d and revealed higher amount of carbohydrates, proteins, lipids, and nucleic acids in spectral data collected from G1 (three days post-burn) in both cases.

Similar findings were obtained comparing G2 \times G3 and G2 \times G4 as shown in Fig. 6. On the other hand, satisfactory data discrimination was not observed in the score plots of G3 \times G4, suggesting that no clear biochemical changes are noticed between spectra from both groups at these days of healing process.

Discussion

Our results using PCA revealed similar biochemical information for the pairwise comparisons G0 \times G1 and G0 \times G2, in which higher content of carbohydrates, proteins, lipids, and nucleic acids were identified in the post-burn groups. These findings indicate intense metabolic activity after the burn trauma and are associated with the cascade of events triggered by the thermal injury. Immediately after the trauma, biological events associated to the homeostasis phase are activated in the wound site. Blood clots are formed on the wound surface to stop the bleeding and migratory cells playing different roles in the healing task are attracted to the region.^{6,49} In our study, no

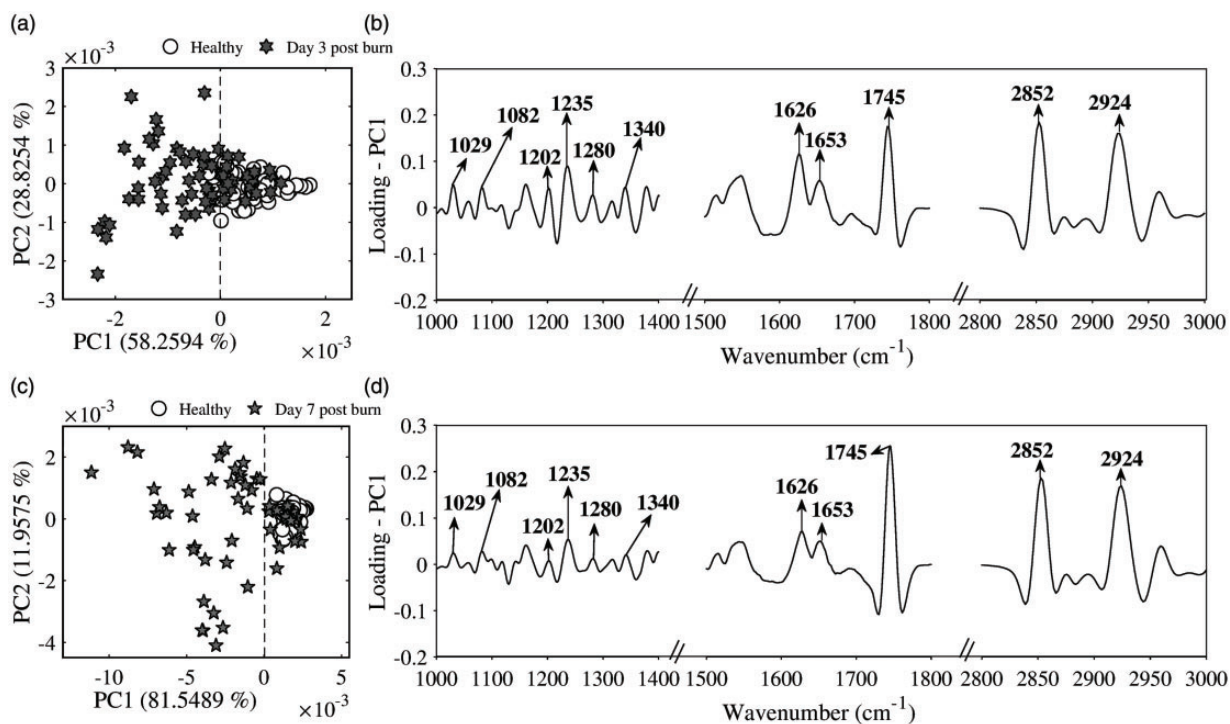


Figure 3. (a,c) PCA score plots obtained by the two main principal components (PC1 \times PC2) for days 3 and 7 compared to healthy tissue. (b,d) Loadings associated to the first principal component obtained by each pairwise comparison (G0 \times G1 and G0 \times G2). White circles represent scores related to spectra of healthy tissue, hexagram and pentagram relate to spectra collected for days 3 and 7 post-burn.

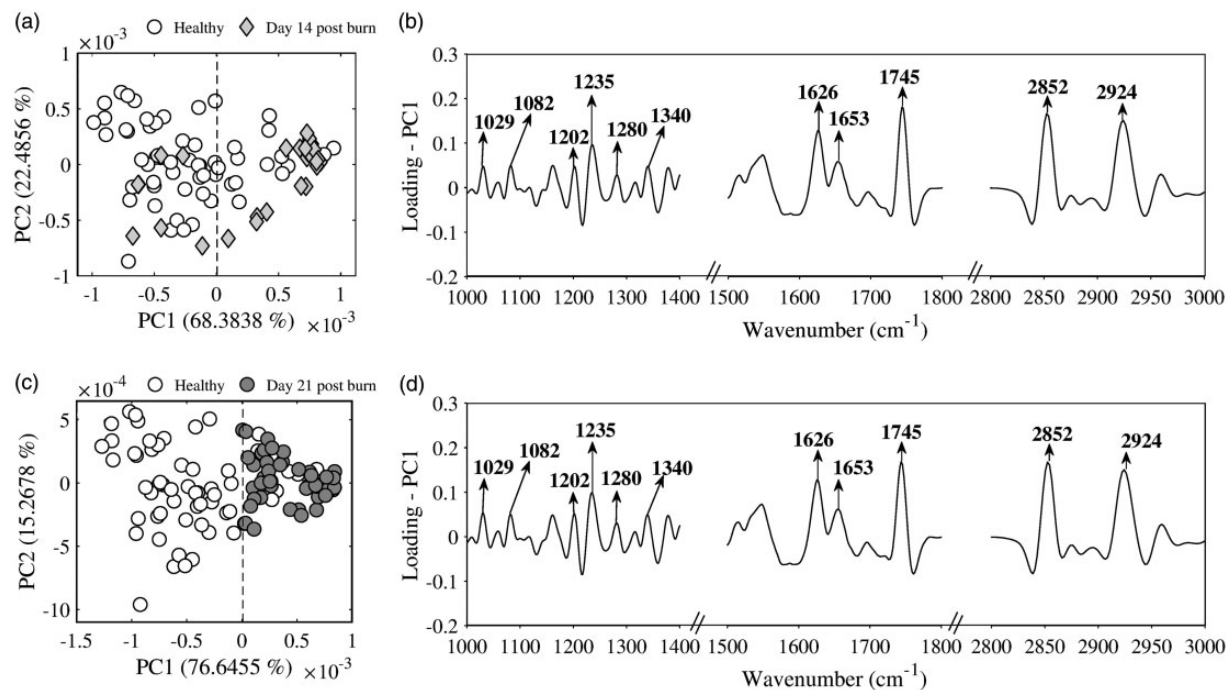


Figure 4. (a,c) Score plots using PC1 and PC2 obtained for G0 \times G3 and G0 \times G4 pairwise comparisons. (b,d) Loadings of PC1. White circles represent scores related to spectra of healthy tissue, diamond and gray circles relate to spectra collected for days 14 and 21 post-burn.

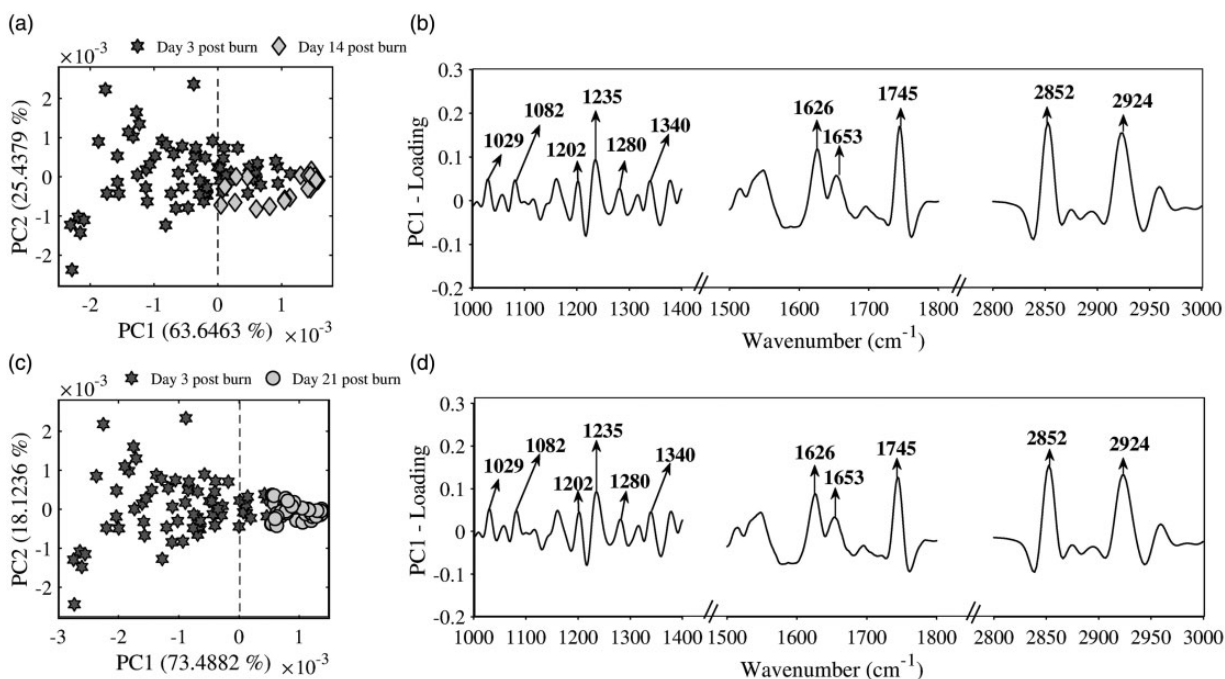


Figure 5. (a,c) Score plots using PC1 and PC2 obtained for G1 × G3 and G1 × G4 pairwise comparisons. (b,d) Loadings of PC1. Black hexagram represents scores related to spectra of day 3 post burn tissue, diamond and gray circles relate to spectra collected for days 14 and 21 post-burn.

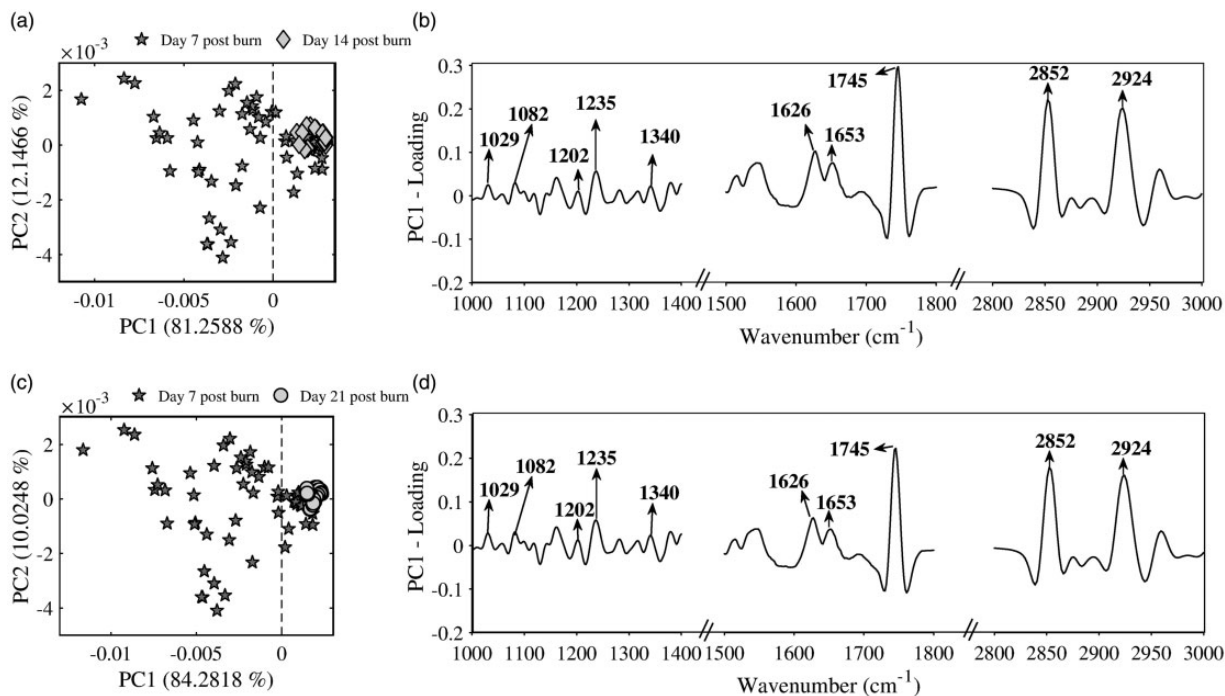


Figure 6. (a,c) Score plots using PC1 and PC2 obtained for G2 × G3 and G2 × G4 pairwise comparisons. (b,d) Loadings of PC1. Gray pentagram represent scores related to spectra of day 7 post-burn tissue, diamond and gray circles relate to spectra collected for days 14 and 21 post-burn.

tissue was extracted immediately after the thermal injury; therefore, the events associated to homeostasis were not evaluated. Concurrent to the homeostasis, growth factors, cytokines, and chemokines released on the wound area activate an inflammatory response, therefore initiating the inflammatory phase.^{6,49} It is important to notice that the biological events associated to the distinct phases that regulate the healing process are overlapped and vary with the severity of the burn trauma (size and depth), location, infection, and other characteristics particular to each individual (age, genetic conditions, etc.).⁷ Thus, there is no consensus about the exact duration of each phase of the wound repair, since this is a multifactorial process influenced by all the factors mentioned above. According to Landen et al., the inflammation in normal skin wound healing usually lasts for 2–5 days after injury.^{6,50} On the other hand, Xue et al. stated that inflammation progresses to the proliferative phase after 2–3 days.⁵¹ In our study, intense inflammatory cell infiltration was evidenced by histological examination after three and seven days of thermal injury, indicating that the inflammatory phase is still ongoing at the seventh day.

Histological aspects of granulation tissue were also observed at three and seven days of wound healing and indicate that proliferative phase has already initiated. Fibroblasts attracted to the wound site synthesize granulation tissue in order to restore the network of blood vessels to provide nutrition and oxygen to the growing healing tissue. Granulation tissue is composed of fibrous proteins such as collagen and elastin,^{6,49} which present vibrational modes over the range 1200–1400 cm^{-1} due to its fibrous structure.⁵¹ Besides these bands, the secondary structure of fibrous proteins also have vibrations peaking at Amide I region. Thus, overexpression of Amide I and the increased absorption of bands peaking at 1202, 1235, 1280, and 1338 cm^{-1} revealed by PCA in the spectra from G1 and G2 indicate the intense synthesis of collagen and elastin demanded to the formation of granulation tissue and extracellular matrix (ECM). The overexpression of sub-bands of Amide I is also influenced by the contribution of non-fibrous proteins playing different roles during the healing process. Granulation tissue is also composed by other ECM components such as glycoproteins, proteoglycans, glycosaminoglycans, and hyaluronic acid.⁶ These molecules are essentially constituted by carbohydrates (monosaccharides, disaccharides, polysaccharides) associated or not to other molecules and have vibrational modes peaking at 1029 and 1082 cm^{-1} . The overexpression of these bands in the spectra of G1 and G2 groups indicate the high demand of these molecular structural units during the wound repair.

Higher amount of lipids were identified by PCA at three and seven days following burn wounding and may reflect the direct involvement of some lipids in cell signaling (such as phosphatidic acid, phosphoinositide, and diacylglycerol)⁵² as well as source of energy (triglycerides, diglycerides, cholesterol, free fat acids) for cell proliferation (growth and

division), migration and for synthesis of cellular matrix.^{53,54} Besides the metabolic and energetic changes induced by the intense proliferation of cells in the wound site during the healing process, an increase in the nucleic acids content may also be expected. In fact, spectral signatures peaking at 1082 and 1235 cm^{-1} , which are associated with symmetric and asymmetric phosphate stretching from nucleic acids, presented overexpression in the spectral data from G1 and G2.

Histological aspects observed at the 14th and 21st days of healing indicated partial and full recovery, respectively. Neither granulation tissue nor inflammatory cell infiltrate was observed in the healing tissue at these days, indicating that proliferative phase has ended and the remodeling phase is in process. At this stage, the collagen III produced in the ECM is replaced by collagen I, the number of new blood vessels decrease, the skin components are restored (hair follicles and sweat glands), and fibroblasts are differentiated into myofibroblasts in order to express as smooth muscle actin that contract the wound.⁶ Fibroblasts were identified in the dermis at the 14th day, but not observed at the 21st day of healing, suggesting that wound contraction is over. At 21 days post-burn, the skin presented histological aspects of normality, therefore indicating that the healing process has ended.

The ability of PCA to discriminate spectral data from different groups is associated to the biochemical level of similarity between the groups compared. No clear biochemical changes were observed by PCA comparing G3 and G4 spectra to each other, which may be an indicative that both groups are in the same healing phase. On the other hand, decreased amounts of carbohydrates, proteins, nucleic acids, and lipids were identified comparing G3 and G4 to G1 and G2, indicating that metabolic activity induced by thermal injury decreases as the healing process progresses. Reduced amounts of tissue molecular units were also evidenced comparing G3 and G4 to G0, suggesting that despite the similar histological aspects, healed tissue is biochemically different of healthy skin.

Determining the state of wound repair is of great importance in deciding the appropriate treatment for a thermally injured patient. However, the current methods used to obtain detailed information about the status of tissue repair are laborious, time-consuming, and expensive. In our study, we demonstrate that FT-IR spectroscopy is able to provide information about the healing status of a wound based on the biochemical information retained by spectral signatures in each phase of healing. Although the method is not capable of identifying specific molecules when compared to molecular tests, as well as assess spatial differences provided by FT-IR imaging, our findings indicate that FT-IR spectroscopy is able to evaluate the progress of tissue repair including full recovery based on the biological events triggered by third-degree burn trauma.

Conclusion

In this study, FT-IR spectroscopy was used to monitor the progress and healing status of cutaneous wounds after third-degree burn trauma. Tissue collected on days 3 and 7 presented higher amounts of carbohydrates, proteins, lipids, and nucleic acids compared to healthy skin, indicating intense metabolic activity at these phases of wound healing. Pairwise comparison of post-burn groups revealed that metabolic activity induced by thermal injury decreases as the healing process progresses. On days 14 and 21 post-burn, healed tissue presented reduced amounts of molecular structural units compared to healthy skin, suggesting that biological events triggered by burn trauma are significantly reduced and the healing process is over. Our findings demonstrate that FT-IR spectroscopy can monitor the biological events triggered by burn trauma as well as to detect the wound repair status including full recovery based on the spectral changes associated to the biochemical events in each phase.

Declaration of Conflicting Interests


The author(s) declared no potential conflicts of interest with respect to the research, authorship, and/or publication of this article.

Funding

This study was supported by FAPESP (CEPID 05/51689-2, 17/50332-0, 13/26113-6), CAPES/PROCAD 88881.068505/2014-01, CNPq (INCT-465763/2014-6, PhD-grant-141946/2018-0 and 141629/2015-0, PQ-309902/2017-7).

ORCID iDs

Pedro Castro  <https://orcid.org/0000-0003-0487-7902>

Denise Zezell  <https://orcid.org/0000-0001-7404-9606>

Supplemental Material

The supplemental material mentioned in the text, consisting of Tables S1 to S4, is available in the online version of the journal.

References

- World Health Organization. "WHO Media Center Fact Sheets: Burns". (2018). <https://www.who.int/news-room/fact-sheets/detail/burns> [accessed Oct 30 (2019)].
- G.G. Pereira, S.S. Guterres, A.G. Balducci, et al. "Polymeric Films Loaded with Vitamin E and *Aloe vera* for Topical Application in the Treatment of Burn Wounds". *BioMed Res. Int.* 2014. 2014: 1–9.
- C. Smolle, J.C. Daniel, A.A. Forbes, et al. "Recent Trends in Burn Epidemiology Worldwide: A Systematic Review". *Burns.* 2017. 43(2): 249–257.
- E.J. Mulholland, N. Dunne, H.O. McCarthy. "MicroRNA as Therapeutic Targets for Chronic Wound Healing". *Mol. Ther. Nucleic Acids.* 2017. 8: 46–55.
- S. Dekoninck, C. Blanpain. "Stem Cell Dynamics, Migration and Plasticity During Wound Healing". *Nat. Cell Biol.* 2019. 21(1): 18–24.
- N.X. Landen, D. Li, M. Stahle. "Transition From Inflammation to Proliferation: A Critical Step During Wound Healing". *Cell. Mol. Life Sci.* 2016. 73(20): 3861–3885.
- B. Magne, J.J. Lataillade, M. Trouillas. "Mesenchymal Stromal Cell Preconditioning: The Next Step Toward a Customized Treatment For Severe Burn". *Stem Cells Dev.* 2018. 27(20): 1385–1405.
- S.A. Eming, P. Martin, M.T. Canic. "Wound Repair and Regeneration: Mechanisms, Signaling, and Translation". *Sci. Transl. Med.* 2014. 6(265): 265–256.
- M. Takeo, W. Lee, M. Ito. "Wound Healing and Skin Regeneration". *Cold Spring Harbor Perspect. Med.* 2015. 5(1): a023267.
- A. Andreoli, M.T. Ruf, G.E. Sopoh, et al. "Immunohistochemical Monitoring of Wound Healing in Antibiotic Treated Buruli Ulcer Patients". *PLoS Neglected Trop. Dis.* 2014. 8(4): e2809.
- J. Zhang, J. Guan, X. Niu, et al. "Exosomes Released From Human Induced Pluripotent Stem Cells-Derived MSCs Facilitate Cutaneous Wound Healing by Promoting Collagen Synthesis and Angiogenesis". *J. Transl. Med.* 2015. 13: 49.
- J.R. Guo, L. Yin, Y.Q. Chen, et al. "Autologous Blood Transfusion Augments Impaired Wound Healing in Diabetic Mice by Enhancing lncRNA H19 Expression via the HIF-1 α Signaling Pathway". *Cell Commun. Signaling.* 2018. 16(1): 84.
- N.S. Greaves, B. Benatar, S. Whiteside, et al. "Optical Coherence Tomography: A Reliable Alternative to Invasive Histological Assessment of Acute Wound Healing in Human Skin". *Br. J. Dermatol.* 2014. 170(4): 840–850.
- R. Jain, D. Calderon, P.R. Kierski, et al. "Raman Spectroscopy Enables Noninvasive Biochemical Characterization and Identification of the Stage of Healing of a Wound". *Anal. Chem.* 2014. 86(8): 3764–3772.
- C.A. Lima, V.P. Goulart, L. Correa, et al. "ATR-FTIR Spectroscopy for the Assessment of Biochemical Changes in Skin Due to Cutaneous Squamous Cell Carcinoma". *Int. J. Mol. Sci.* 2015. 16(4): 6621–6230.
- C.A. Lima, V.P. Goulart, L. Correa, et al. "Using Fourier Transform Infrared Spectroscopy to Evaluate Biological Effects Induced by Photodynamic Therapy". *Lasers Surg. Med.* 2016. 48(5): 538–545.
- K.P. Quinn, K.E. Sullivan, Z. Liu, et al. "Optical Metrics of the Extracellular Matrix Predict Compositional and Mechanical Changes after Myocardial Infarction". *Sci. Rep.* 2016. 6: 35823.
- M.O.D. Santos, A. Latrive, P.A.A. Castro, et al. "Multimodal Evaluation of Ultra-Short Laser Pulses Treatment for Skin Burn Injuries". *Biomed. Opt. Express.* 2017. 8(3): 1575–1588.
- D. Ami, P. Mereghetti, A. Foli, et al. "ATR-FTIR Spectroscopy Supported by Multivariate Analysis for the Characterization of Adipose Tissue Aspirates from Patients Affected by Systemic Amyloidosis". *Anal. Chem.* 2019. 9(4): 2894–900.
- M.J. Baker, J. Trevisan, P. Bassan, et al. "Using Fourier Transform IR Spectroscopy to Analyze Biological Materials". *Nat. Protoc.* 2014. 9(8): 1771–1791.
- M. Diem, A. Mazur, K. Lenau, et al. "Molecular Pathology via IR and Raman Spectral Imaging". *J. Biophotonics.* 2013. 6(11–12): 855–886.
- A.C.S. Talari, M.A.G. Martinez, Z. Movasaghi, et al. "Advances in Fourier Transform Infrared (FTIR) Spectroscopy of Biological Tissues". *Appl. Spectrosc. Rev.* 2016. 52(5): 456–506.
- M. Paraskevaidi, C.L.M. Morais, K.M.G. Lima, et al. "Differential Diagnosis of Alzheimer's Disease Using Spectrochemical Analysis of Blood". *Proc. Natl. Acad. Sci. U. S. A.* 2017. 114(38): E7929–E7938.
- S. Roy, D.P. Guaita, D.W. Andrew, et al. "Simultaneous ATR-FTIR Based Determination of Malaria Parasitemia, Glucose and Urea in Whole Blood Dried onto a Glass slide". *Anal. Chem.* 2017. 89(10): 5238–5245.
- M.J. Baker, H.J. Byrne, J. Chalmers, et al. "Clinical Applications of Infrared and Raman Spectroscopy: State of Play and Future Challenges". *Analyst.* 2018. 143(8): 1735–1757.
- P.L. Fale, A. Altharawi, K.L. Chan. "In situ Fourier transform infrared analysis of live cells' response to doxorubicin". *Biochim. Biophys. Acta.* 2015. 1853(10): 2640–2648.
- S. Kalmodia, S. Parameswaran, W. Yang, et al. "Attenuated Total Reflectance Fourier Transform Infrared Spectroscopy: An Analytical

- Technique to Understand Therapeutic Responses at the Molecular Level". *Sci. Rep.* 2015. 5: 16649.
28. A.L.B. Carvalho, M. Pilling, P. Gardner, et al. "Chemotherapeutic Response to Cisplatin-like Drugs in Human Breast Cancer Cells Probed by Vibrational Microspectroscopy". *Faraday Discuss.* 2016. 187: 273–298.
 29. E. Giorgini, S. Sabbatini, R. Rocchetti, et al. "In vitro FTIR Microspectroscopy Analysis of Primary Oral Squamous Carcinoma Cells Treated with Cisplatin and 5-Fluorouracil: A New Spectroscopic Approach for Studying the Drug–Cell Interaction". *Analyst.* 2018. 143(14): 3317–3326.
 30. S.B. White, M. Romeo, T. Chernenko, et al. "Cell-Cycle-Dependent Variations in FTIR Micro-Spectra of Single Proliferating HeLa Cells: Principal Component and Artificial Neural Network Analysis". *Biochim. Biophys. Acta.* 2006. 1758(7): 908–914.
 31. U. Zelig, J. Kapelushnik, R. Moreh, et al. "Diagnosis of Cell Death by Means of Infrared Spectroscopy". *Biophys. J.* 2009. 97(7): 2107–2114.
 32. A. Pieliesz, D. Biniás, E. Sarna, et al. "Active Antioxidants in Ex-Vivo Examination of Burn Wound Healing by Means of IR and Raman Spectroscopies – Preliminary Comparative Research". *Spectrochim. Acta, Part A.* 2017. 173: 924–930.
 33. G.J.V. Zapien, M.M.M. Miranda, F.J.G. Sanchez, et al. "Biomolecular Characterization by FTIR Microspectroscopy in the Modeling Phase of Wound Cicatrization in a Murine Model of Excisional Injury". *Int. J. Morphology.* 2019. 37(4): 1234–1244.
 34. N.J. Crane, E.A. Elster. "Vibrational Spectroscopy: A Tool Being Developed for the Noninvasive Monitoring of Wound Healing". *J. Biomed. Opt.* 2012. 17(1): 010902.
 35. K.L.A. Chan, G. Zhang, M.T. Canic, et al. "A Coordinated Approach to Cutaneous Wound Healing: Vibrational Microscopy and Molecular Biology". *J. Cell. Mol. Med.* 2008. 12(5b): 2145–2154.
 36. W.A. Dorsett-Martin, A.B. Wysocki. "Rat Models of Skin Wound Healing". In: P.M. Conn, editor. *Sourcebook of Models for Biomedical Research.* New Jersey, USA: Humana Press, 2008.
 37. A. Abdullahi, S.A. Nik, M.G. Jeschke. "Animal Models in Burn Research". *Cell. Mol. Life Sci.* 2014. 71(17): 3241–3255.
 38. S. Liyanage, A. Noureddine. "Fourier Transform Infrared Applications to Investigate Induced Biochemical Changes in Liver". *Appl. Spectrosc. Rev.* 2019. 1–33. DOI: 10.1080/05704928.2019.1692307.
 39. J. Filik, M.D. Froglev, J.K. Pijanka, et al. "Electric Field Standing Wave Artefacts in FTIR Micro-Spectroscopy of Biological Materials". *Analyst.* 2012. 137: 853–861.
 40. S.G. Kazarian, K.L.A. Chan. "ATR-FTIR Spectroscopic Imaging: Recent Advances and Applications to Biological Systems". *Analyst.* 2013. 138: 1940–1951.
 41. P. Bassan, A. Sachdeva, J. Lee, et al. "Substrate Contributions in Micro-ATR of Thin Samples: Implications for Analysis of Cells, Tissue and Biological Fluids". *Analyst.* 2013. 38: 4139–4146.
 42. K.L.A. Chan, S.G. Kazarian. "Correcting the Effect of Refraction and Dispersion of Light in FT-IR Spectroscopic Imaging in Transmission through Thick Infrared Windows". *Anal. Chem.* 2013. 85: 1029–1036.
 43. L. Cui, H.J. Butler, P.L.M. Hirsch, et al. "Aluminium Foil as a Potential Substrate for ATR-FTIR, Transflection FTIR or Raman Spectrochemical Analysis of Biological Specimens". *Anal. Methods.* 2016. 8(3): 481–487.
 44. C.L.M. Morais, M. Paraskevaidi, L. Cui, et al. "Standardization of Complex Biologically Derived Spectrochemical Datasets". *Nat. Protoc.* 2019. 14(5): 1546–1577.
 45. J. Nallala, O. Piot, M.D. Diebold, et al. "Infrared Imaging as a Cancer Diagnostic Tool: Introducing a New Concept of Spectral Barcodes for Identifying Molecular Changes in Colon Tumors". *Cytometry Part A.* 2013. 83A(3): 294–300.
 46. Z. Movasaghi, S. Rehman, I.U. Rehman. "Fourier Transform Infrared (FTIR) Spectroscopy of Biological Tissues". *Appl. Spectrosc. Rev.* 2008. 43(2): 134–179.
 47. M. Diem. "Appendix F: Infrared and Raman Spectra of Selected Cellular Components". In: *Modern Vibrational Spectroscopy and Micro-Spectroscopy.* Northeastern University, USA: John Wiley and Sons, 2015. pp. 399–403.
 48. K. Belbachir, R. Noreen, G. Gouspillou, et al. "Collagen Types Analysis and Differentiation by FTIR Spectroscopy". *Anal. Bioanal. Chem.* 2009. 395(3): 829–837.
 49. H.A. Owida, A.V. Rutter, G. Cinque, et al. "Vibrational Spectroscopic Monitoring and Biochemical Analysis of Pericellular Matrix Formation and Maturation in a 3-Dimensional Chondrocyte Culture Model". *Analyst.* 2018. 143(24): 5979–5986.
 50. V.L. Kozel'tsev, T.V. Volodina, A.N. Pankrushina, et al. "Changes in Wound Field Lipids in Rat Skin". *Bull. Exp. Biol. Med.* 2006. 142(4): 493–494.
 51. M. Xue, C.J. Jackson. "Extracellular Matrix Reorganization During Wound Healing and Its Impact on Abnormal Scarring". *Adv. Wound Care (New Rochelle).* 2015. 4(3): 119–136.
 52. J.J. Hew, R.J. Parungao, H. Shi, et al. "Mouse Models in Burns Research: Characterisation of the Hypermetabolic Response to Burn Injury". *Burns.* 2019. PII: S0305-4179(19)30434-6. DOI: 10.1016/j.burns.2019.09.014.
 53. R. Cheheltani, C.M. McGoverin, J. Rao, et al. "Fourier Transform Infrared Spectroscopy to Quantify Collagen and Elastin in an in Vitro Model of Extracellular Matrix Degradation in Aorta". *Analyst.* 2014. 139(12): 3039–3047.
 54. G. Yu, O. Stojadinovic, M.T. Canic, et al. "Infrared Microscopic Imaging of Cutaneous Wound Healing: Lipid Conformation in the Migrating Epithelial Tongue". *J. Biomed. Opt.* 2012. 17(9): 96009–1.